

# Seismic Inclined Pull-out Capacity of Vertical Strip Anchors

Farzana S. Nadaf<sup>1</sup> Sunil M. Rangari<sup>2</sup>

<sup>1</sup>Research Scholar <sup>2</sup>Professor and Head

<sup>1,2</sup>Department of Civil Engineering

<sup>1,2</sup>Saraswati Collage of Engineering, Maharashtra, India

**Abstract**— This present paper studied the behaviour of the vertical strip anchors subjected to inclined load. Calculation of soil reaction on failure surfaces is computed by using Kötter's equation (1903). Separate analysis is carried out for both active and passive zone of failure. It also includes formulations for pseudo-static analysis. Derivations are described to find inclined pull-out factor by using limit equilibrium method. The angle of failure planes are optimized to obtain the inclined pull-out capacity of vertical strip anchors by using pseudo-static approaches. The results obtained from the study are tabulated and effect of various parameters are discussed in detail and presented in tabular and graphical form. In this study approaches for estimation of inclined pull-out capacity of vertical plate anchors are reviewed.

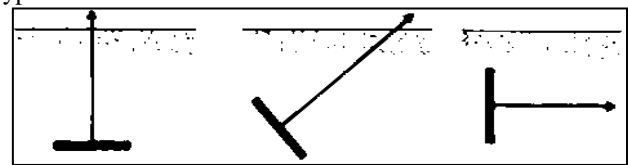
**Key words:** Pullout Capacity, Inclined Loading, Vertical Plate Anchors

## I. INTRODUCTION

Foundations of many structures are frequently subjected to vertical pullout or inclined outward forces. Design of such foundations, may be done through the use of tension members. These members tries to come out of the ground, hence these are sufficiently embedded into the soil to resist these outward forces, are called the ground anchors/earth anchors. Ground anchors can be used for temporary or permanent applications for resisting action of flood, wind, and seismic forces. The strength of ground anchor is attained through the shearing resistance developed along the failure surfaces and the weight of soil in the failure zone. There are various types of ground anchors which are used to resist uplift forces/outward forces; anchors embedded in soil can be divided into five basic categories (Das, 1990): plate anchors, screw anchors, direct embedment anchors, grouted anchors and pile anchor.

Ground anchors are the tension members in which the direction can be horizontal, inclined or vertical as shown in figure 1.1. The plate anchors may be horizontal to resist vertically-directed uplifting load, inclined to resist axial pullout load, or vertical to resist horizontally-directed pullout load. The materials used for plate anchors may be steel plates, precast concrete slabs, poured concrete slabs, timber sheets, and so forth. The more usual shapes of plate anchors are circular, rectangular, square and strip. In this thesis, plate anchors are analyzed broadly for obtaining their pullout capacities under both static and seismic conditions. The plate anchor can be installed in the excavated trench of required depth and then backfilling and compacting the soil of adequate quality. Load can be transferred to the soil through direct bearing in case of plate anchors, whereas load transfer mechanism is different for rest of the ground anchors. Offshore and on shore structures are subjected to pullout load. Design of transmission towers, suspension cable bridges, jetties requires the study of estimating the pullout capacity.

The current work deals with the pullout capacity of embedded vertical anchors. Vertical anchors are used for earth-retaining structures and foundations of soil supported structures. Use of earth anchors in construction is for transmitting the outwardly-directed load to the soil at a greater depth or away from the structure which is the fundamental reason behind the utility of the anchors. Anchors help in such a way that the outwardly directed loads are transmitted to soil at a considerably greater depth. Figure 1.1 represents different types of anchors embedded in the soil.



(a) Horizontal anchor (b) Inclined anchor (c) Vertical Anchor

Fig. 1.1: Plate Anchors

## II. METHODOLOGY

The main aim of the study is to obtain pullout capacity of vertical strip anchor in both static and seismic conditions subjected to inclined load.

### A. Formulations for Pseudo-Static Analysis

Figures 2.3 shows a shallow vertical strip anchor with inclined load embedded in a homogeneous cohesion less soil. The objective is to find the pullout capacity of these anchors. A vertical strip anchor, as shown in Fig. 2.3, of height,  $B$  and embedded by depth,  $H$  below the ground surface, is subjected to a inclined pull,  $P_{ud}$ . The analysis is carried out to calculate the  $P_{ud}$ , acting on the anchor by considering the pseudo-static forces acting on vertical strip anchor and shown in Fig. 2.3.

When the failure occurs in the soil mass due to inclined pull of the anchor, there occur two failure surfaces, which are described below in (Fig2.4):

- The failure surface,  $AE$ , is assumed to be a straight line, which passes through the base of the anchor. For the calculation of forces on this failure surface, Kötter's equation (1903) for the active earth pressure state is used.
- The failure surface,  $DF$ , which passes through the base of the anchor and is in front of the anchor plate, is in a state of plastic equilibrium and passive condition prevails in the soil. Kötter's equation (1903) for passive earth pressure is used for the calculation of the forces on this failure surface.

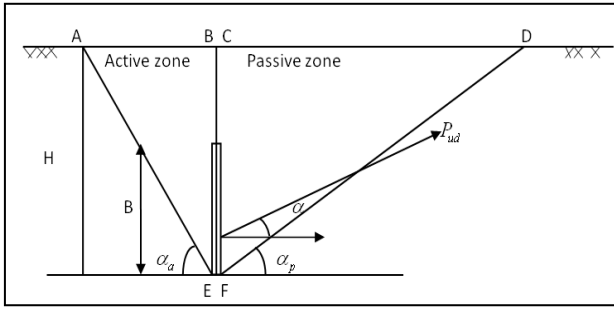


Fig. 2.3: Shallow Vertical Strip Anchor with Planar Failure Surfaces

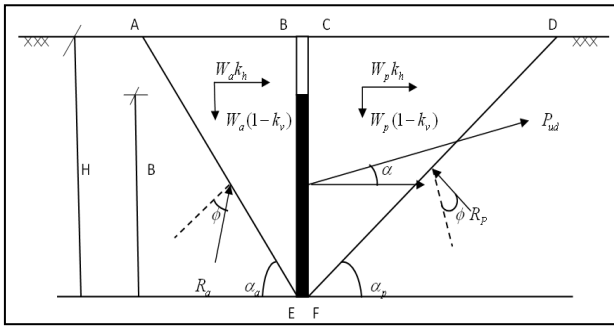


Fig. 2.4: Pseudo Static Forces on Vertical Strip Anchor

$W_a$  = The weight of active failure wedge ABE, in active case,  
 $W_p$  = The weight of, failure wedge, CDF, in passive case,  $k_h$  =  
 seismic coefficient's in horizontal direction,  $k_v$  = The seismic  
 coefficient in vertical direction,  $\phi$  = Angle of internal friction,  
 $B$  = width of vertical strip anchor,  $H$  = height of vertical strip  
 anchor below ground surface,  
 $R_a$  = The reaction exerted by the soil to the failure surface AE,  
 $R_p$  = The reaction exerted by the soil to the failure surface DF,  
 $\alpha_a$  =, an angle made by failure surface in active case,  $\alpha_p$  =,  
 an angle made by failure surface in passive case.

### B. Analysis for Active Zone

The weight of failure wedge ABE is  $W_a$  is acted upon by following forces and is shown in fig. 3.5 The seismic coefficient's in horizontal and vertical direction are represented by  $K_h$  and  $K_v$  respectively. The reaction,  $R_a$  exerted by the soil to the failure surface AE making an angle  $\phi$  and is inclined at an angle  $\alpha_a$  and is inclined at an angle  $\delta$ , with the normal to the anchor.

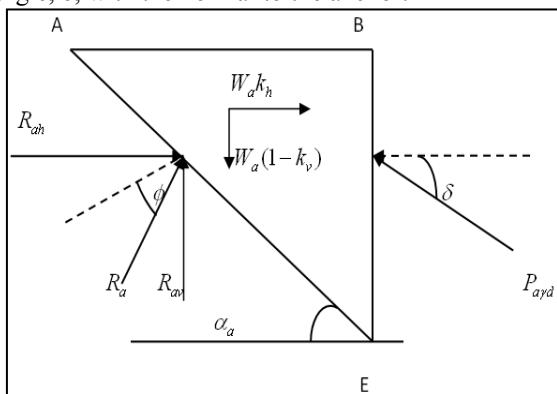


Fig. 3.5: Free Body Diagram of Failure Wedge in Active Case

The weight of soil mass ABE is given by,

$$W_a = \frac{\gamma H^2}{2 \tan \alpha_a} \quad (2.5)$$

For plane failure surface, Kotter's equation (1903) for the active case can be written as,

$$\frac{dp}{ds} = \gamma \sin(\alpha_a - \phi) \quad (2.6)$$

Solving the differential equation, the pressure distribution,  $p$ , on the failure surface is given by,

$$p = \gamma \sin(\alpha_a - \phi) S \quad (2.7)$$

Thus the reaction  $R_a$  exerted by the rest of the soil to the failure surface AE is given by,

$$R_a = \int_0^{BF} P_1 ds \quad (2.8)$$

$$R_a = \int_0^{BF} \gamma \sin(\alpha_a - \phi) s ds \quad (2.9)$$

$$R_a = \frac{\gamma BF^2}{2} \sin(\alpha_a - \phi) \quad (2.10)$$

$$BF = \frac{H}{\sin \alpha_a} \quad (2.11)$$

$$BF^2 = \frac{H^2}{\sin^2 \alpha_a} \quad (2.12)$$

The reaction  $R_a$ , exerted by the rest of soil to the failure surface, AE, is given by,

$$R_a = \frac{\gamma}{2} \frac{H^2}{\sin^2 \alpha_a} \sin(\alpha_a - \phi) \quad (2.13)$$

The active pressure  $P_{ayd}$  can be computed using equation of equilibrium in horizontal and vertical directions and can be written as,

$$\sum F_x = 0$$

$$P_{ayd} = [R_a \sin(\alpha_a - \phi) + W_a k_h] / \cos \delta \quad (2.14)$$

$$\sum F_y = 0$$

$$P_{ayd} = -R_a \cos(\alpha_a - \phi) + W_a (1 - k_v) / \sin \delta \quad (2.15)$$

### C. Analysis of Passive Zone

The failure wedge in passive case, CDF, of weight,  $W_p$  experiences the pseudo-static forces (fig. 2.6). The passive thrust,  $P_{pyd}$ , exerted by the anchor on to the backfill inclined at an angle,  $\delta$ , with normal to the anchor.

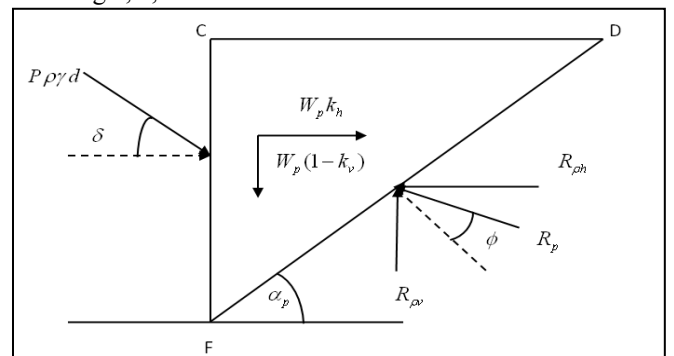


Fig. 3.6: Free Body Diagram of Failure Wedge for Passive Case

The weight,  $W_p$  of the soil wedge, CDF, can be written as,

$$W_p = \frac{\gamma H^2}{2 \tan a_p} \quad (2.16)$$

$$\frac{dp}{ds} = \gamma \sin(a_p + \phi) \quad (2.17)$$

$$p = \gamma \sin(a_p + \phi) S \quad (2.18)$$

The reaction,  $R_p$ , exerted by the soil on to the failure surface, DF, is given by,

$$R_p = \int_0^{CF} p_1 ds \quad (2.19)$$

$$R_p = \int_0^{CF} \gamma \sin(a_p + \phi) s ds \quad (2.20)$$

$$CF = \frac{H}{\sin a_p} \quad (2.21)$$

$$CF^2 = \frac{H^2}{\sin^2 a_p} \quad (2.22)$$

$$R_p = \frac{\gamma}{2} \frac{H^2}{\sin^2 a_p} \sin(a_p + \phi) \quad (2.23)$$

$$\sum F_x = 0$$

$$P_{pyd} \cos \delta + W_p K_h = R_{ph} \sin(a_p + \phi)$$

$$P_{pyd} = [R_p \sin(a_p + \phi) - W_p k_h] / \cos \delta \quad (2.24)$$

$$\sum F_y = 0$$

$$P_{pyd} \sin \delta + W_p (1 - k_v) = R_p \cos(a_p + \phi)$$

$$P_{pyd} = [R_p \sin(a_p + \phi) - W_p (1 - k_v)] / \sin \delta \quad (2.25)$$

Calculation of Angle of failure planes:-

Take equation in seismic conditions, angle of failure planes changes with change in values of seismic acceleration coefficients in both horizontal and vertical directions in addition to soil friction angle (Rangari et al., 2013). Hence, a rigorous trial and error procedure is used in the present analysis to optimize the critical angle of the failure planes until a convergence is reached to the third decimal.

The trial values obtained for  $\alpha_a$  must satisfy the condition where by the two computed values for  $P_{ayd}$  from Eq. (2.14) and Eq. (2.15) should be same. Similarly, values of  $\alpha_p$  are obtained such that two computed values of  $P_{pyd}$  must satisfy the force equilibrium conditions from Eq. (2.24) and Eq. (2.25).

The angle of active and passive failure can be obtained by using the Eq. (2.28) and Eq. (2.33) respectively,

$$\left[ \frac{\sin^2(a_a - \phi)}{\sin^2 a_a} + \frac{k_h}{\tan a_a} \right] \tan \delta = \left[ \frac{\sin 2(a_a - \phi)}{2 \sin^2 a_a} + \frac{(1 - k_v)}{\tan a_a} \right] \quad (2.28)$$

$$\left[ \frac{\sin^2(a_p + \phi)}{\sin^2 a_p} - \frac{k_h}{\tan a_p} \right] \tan \delta = \left[ \frac{\sin^2(a_p + \phi)}{\sin^2 a_p} - \frac{(1 - k_v)}{\tan a_p} \right] \quad (2.33)$$

#### 2.4.4 Seismic pullout Capacity

Consider the free body diagram of the vertical strip anchor placed at shallow depth as shown in fig. (2.7).

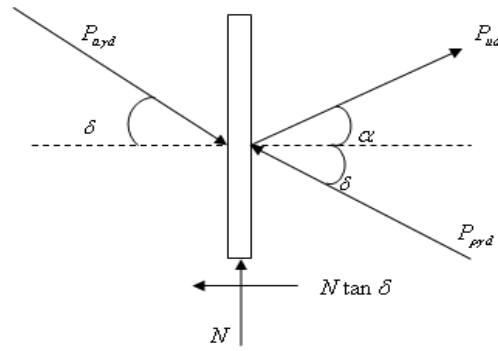


Fig.2.7: Free body diagram of the vertical strip anchor

$$\sum F_y = 0$$

$$N + P_{pyd} \sin \delta + P_{ayd} \sin \delta + P_{ud} \sin \alpha = 0 \quad (2.34)$$

$$N + (P_{pyd} - P_{ayd}) \sin \delta + P_{ud} \sin \alpha \quad (2.35)$$

$$N = (P_{pyd} - P_{ayd}) \sin \delta - P_{ud} \sin \alpha \quad (2.36)$$

$$\sum F_x = 0$$

$$P_{ayd} \cos \delta - P_{pyd} \cos \delta + P_{ud} \cos \alpha - N \tan \delta = 0 \quad (2.37)$$

Put value of N in above equation (3.37)

$$P_{ud} \cos \alpha = P_{pyd} \cos \delta - P_{ayd} \cos \delta + [(P_{pyd} - P_{ayd}) \sin \delta - P_{ud} \sin \alpha] \tan \delta \quad (2.38)$$

$$P_{ud} = \frac{(P_{pyd} - P_{ayd})(\cos \delta - \sin \delta \tan \delta)}{\cos \alpha} \times \frac{1}{(1 + \tan \alpha \tan \delta)}$$

One can write the pullout resistance in non-dimensional form as,

$$F_{yd} = 0.5 \gamma H^2 \left[ \frac{\left( \frac{\sin^2(\alpha_p + \phi)}{\sin^2 \alpha_p} - \frac{\sin^2(\alpha_a - \phi)}{\sin^2 \alpha_a} + K_h \left( \frac{1}{\tan \alpha_a} - \frac{1}{\tan \alpha_p} \right) \right)}{\left( \frac{\sin(\alpha_p + \phi)}{\sin^2 \alpha_p} \cos(\alpha_p + \phi) + \frac{\sin(\alpha_a - \phi) \cos(\alpha_a - \phi)}{\sin^2 \alpha_a} \right)} \right] \times \frac{\tan \delta}{[\cos \alpha (1 + \tan \alpha \tan \delta)]}$$

$$- \left[ \frac{1}{\tan \alpha_a} - \frac{1}{\tan \alpha_p} \right] \right]$$

### III. RESULTS & DISCUSSION

#### A. Results under Pseudo-Static Condition

In case of a dry cohesion-less soils, to avoid the phenomenon of shear fluidization for certain combinations of  $k_h$  and  $k_v$ , values of  $\phi$  considered as per Richards et al. (1990) given as;

$$\phi = \tan^{-1} [k_h / (1 - k_v)] \quad (3.1)$$

Results for the critical angle of failure planes, earth pressure coefficients and seismic pullout capacity factors for vertical strip anchor for inclined load are presented in the form of table for different input parameters are;

Soil friction angle;  $\phi = 10^\circ, 20^\circ, 30^\circ$  and  $40^\circ$ .

Horizontal seismic acceleration coefficient;  $k_h = 0, 0.1, 0.2, 0.3, 0.4$  and  $0.5$ .

Vertical seismic acceleration coefficient;  $k_v = 0, 0.5k_h$  and  $1.0k_h$

Embedment ratio  $\varepsilon = 1, 3, 5,$  and  $7.$

Soil-anchor interface wall friction angle;  $\delta = \phi / 2, 2 \phi / 3, \phi$

Angle of inclined load,  $\alpha = 15^\circ, 30^\circ$  and  $45^\circ$

Seismic pullout factor ( $F_{yd}$ ) shown in Table 4.1 to Table 4.12 is obtained for various combinations of  $k_h$  and  $k_v$  for different values of  $\phi$  and  $\varepsilon$  with  $\delta = \phi / 2, 2 \phi / 3$  and  $\phi$  for load inclination of  $15^\circ, 30^\circ$  and  $45^\circ$

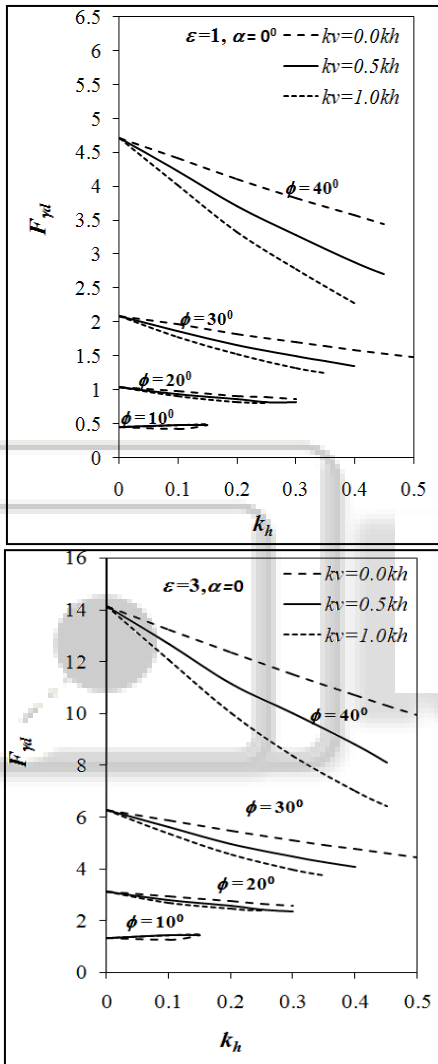
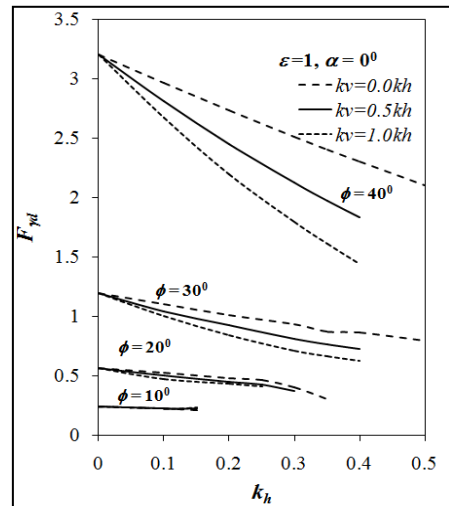
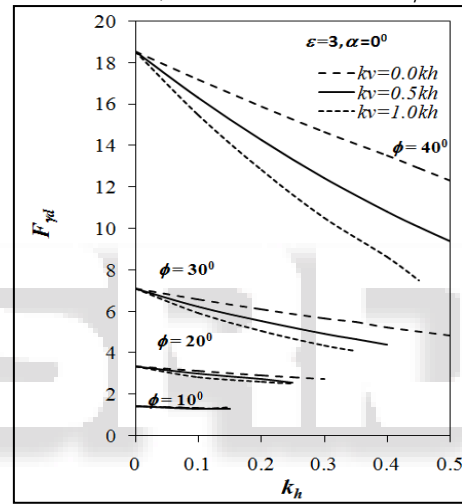


Fig. 3.1: Variation of  $F_{yd}$  with  $k_h$  for various values of  $k_v, \alpha = 0^\circ$  and  $\varepsilon$  with  $\delta = \phi/2$



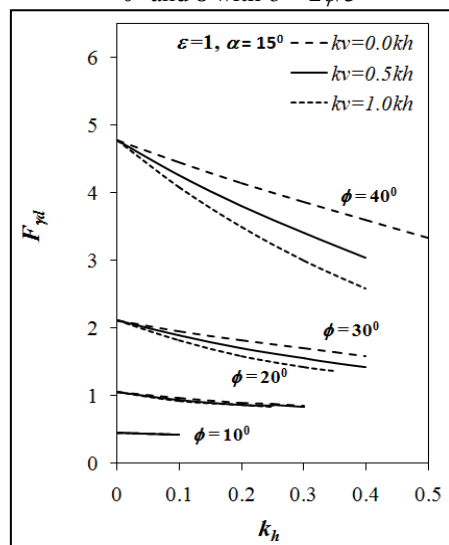
(a)

Fig. 3.2: Variation of  $F_{yd}$  with  $k_h$  for various values of  $k_v, \alpha = 0^\circ$  and  $\varepsilon$  with  $\delta = 2 \phi/3$



(b)

Fig. 3.3: Variation of  $F_{yd}$  with  $k_h$  for various values of  $k_v, \alpha = 0^\circ$  and  $\varepsilon$  with  $\delta = 2 \phi/3$



(a)

Fig. 3.4: Variation of  $F_{yd}$  with  $k_h$  for various values of  $k_v, \alpha = 15^\circ, \phi$  and  $\varepsilon$  with  $\delta = \phi/2$

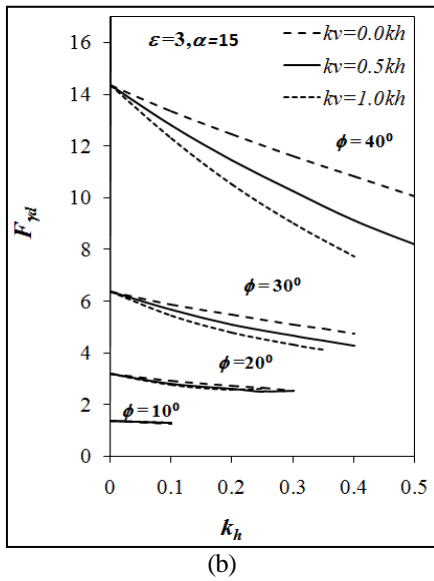


Fig. 3.5: Variation of  $F_{yd}$  with  $k_h$  for various values of  $k_v$ ,  $\alpha = 15^\circ$ ,  $\phi$  and  $\epsilon$  with  $\delta = \phi/2$

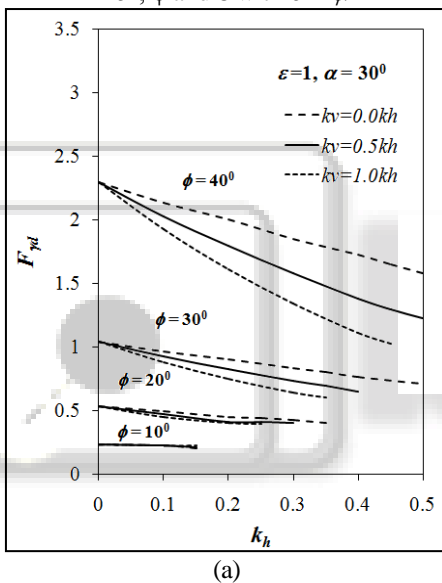


Fig. 3.6: Variation of  $F_{yd}$  with  $k_h$  for various values of  $k_v$ ,  $\alpha = 30^\circ$  and  $\epsilon$  with  $\delta = \phi/2$

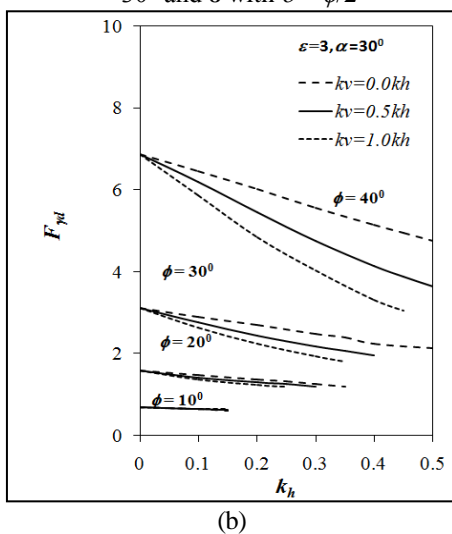


Fig. 3.7: Variation of  $F_{yd}$  with  $k_h$  for various values of  $k_v$ ,  $\alpha = 30^\circ$  and  $\epsilon$  with  $\delta = 2\phi/3$

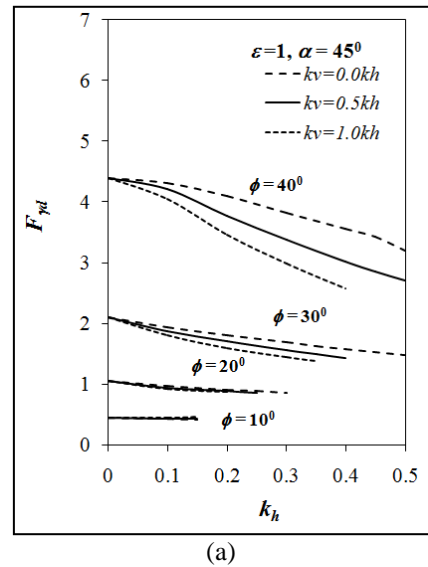


Fig. 3.8: Variation of  $F_{yd}$  with  $k_h$  for various values of  $k_v$ ,  $\alpha = 45^\circ$  and  $\epsilon$  with  $\delta = \phi/2$

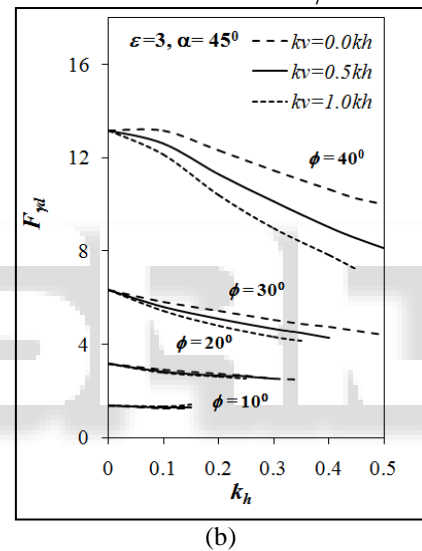


Fig. 3.9: Variation of  $F_{yd}$  with  $k_h$  for various values of  $k_v$ ,  $\alpha = 45^\circ$  and  $\epsilon$  with  $\delta = \phi/2$

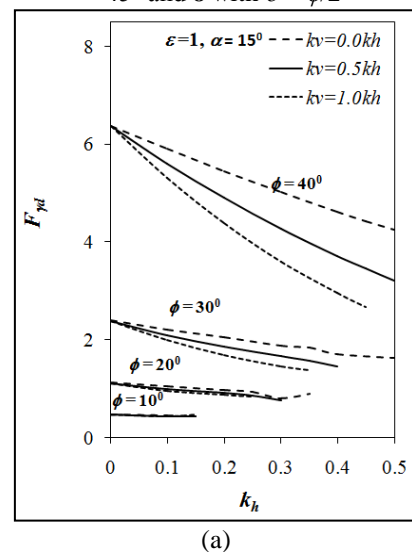
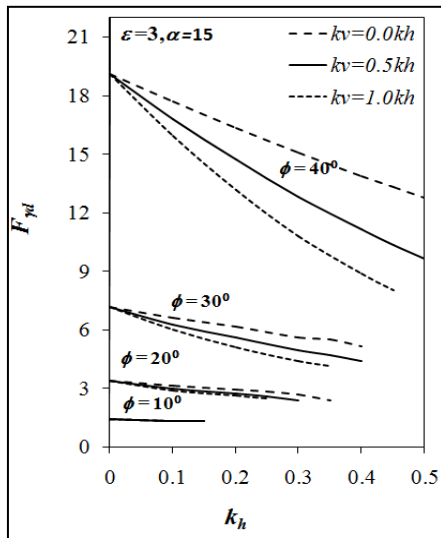
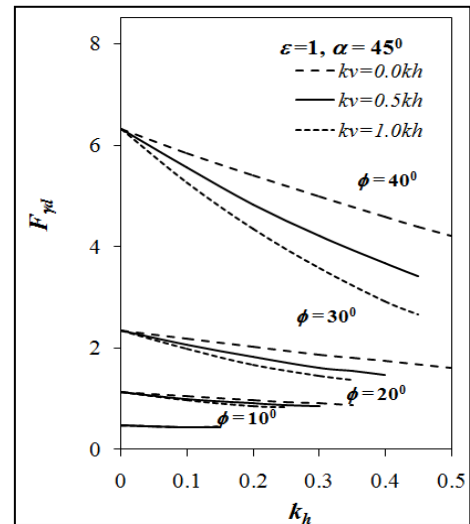


Fig. 3.10: Variation of  $F_{yd}$  with  $k_h$  for various values of  $k_v$ ,  $\alpha = 15^\circ$  and  $\epsilon$  with  $\delta = 2\phi/3$



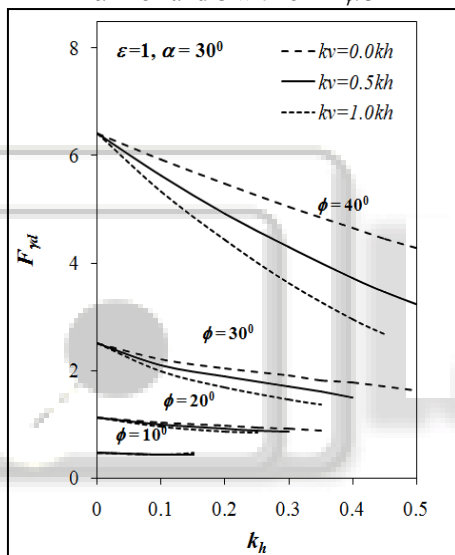
(b)

Fig. 3.11: Variation of  $F_{\gamma d}$  with  $k_h$  for various values of  $k_v$ ,  $\alpha = 15^\circ$  and  $\epsilon$  with  $\delta = 2\phi/3$



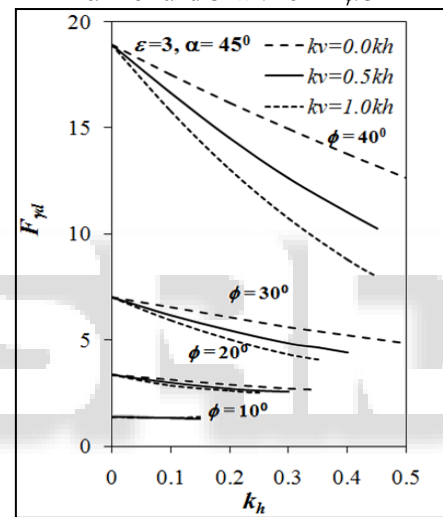
(a)

Fig. 3.14: Variation of  $F_{\gamma d}$  with  $k_h$  for various values of  $k_v$ ,  $\alpha = 45^\circ$  and  $\epsilon$  with  $\delta = 2\phi/3$



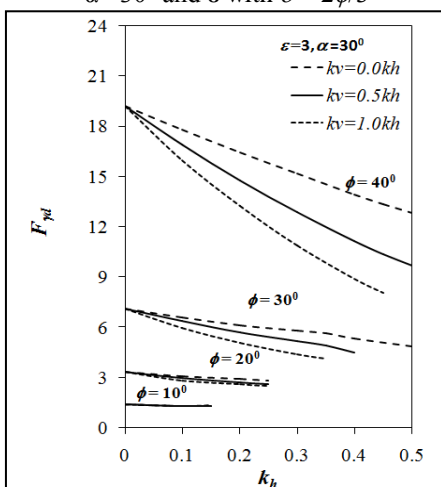
(a)

Fig. 3.12: Variation of  $F_{\gamma d}$  with  $k_h$  for various values of  $k_v$ ,  $\alpha = 30^\circ$  and  $\epsilon$  with  $\delta = 2\phi/3$



(b)

Figure 3.15: Variation of  $F_{\gamma d}$  with  $k_h$  for various values of  $k_v$ ,  $\alpha = 45^\circ$  and  $\epsilon$  with  $\delta = 2\phi/3$



(b)

Fig. 3.13: Variation of  $F_{\gamma d}$  with  $k_h$  for various values of  $k_v$ ,  $\alpha = 30^\circ$  and  $\epsilon$  with  $\delta = 2\phi/3$

### B. Comparison of Results due to Different Inclination of Load

Rangari and Joshi (2016) proposed the values of horizontal pullout capacity used here to find the variation in  $F_{\gamma d}$  with change in load inclination. It is observed that  $F_{\gamma d}$  significantly decreases with increase in  $\alpha$  from 0 to 15° and further increase in load inclination marginal changes (about 3%) are noticed from fig. 3.9. From graph it is worth to note that for  $k_h = 0.2$ ,  $k_v = 0.0k_h$ ,  $\phi = 10^\circ, 20^\circ, 30^\circ$  and  $\epsilon = 3$ ;  $F_{\gamma d}$  decreases by 0.81% for  $\alpha = 15^\circ$ , 0.65% for  $\alpha = 30^\circ$ , 0.49% for  $\alpha = 45^\circ$ , when compared with horizontal pullout. Again from graph it is seen that  $F_{\gamma d}$  decreases to 0.59% for  $\alpha = 15^\circ$ , 0.59% for  $\alpha = 30^\circ$ , 0.59% for  $\alpha = 45^\circ$ , when compared with the values obtained for  $\alpha = 15^\circ$  in presence of  $k_v$ . The values of  $F_{\gamma d}$  slightly increases with increase in load inclination for  $k_v = 0$  and almost same when  $k_v$  increases.

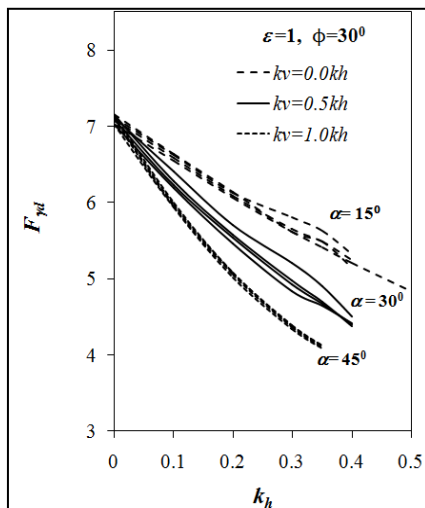


Fig. 3.16: Variation of  $F_{\gamma d}$  with  $k_h$  for various values of  $k_v$ ,  $\phi=30^\circ$  and  $\varepsilon=3$  with  $\delta=2\phi/3$

#### IV. CONCLUSIONS

- 1) Seismic pullout capacity  $F_{\gamma d}$  increases with increase in soil friction angle,  $\phi$ .
- 2)  $F_{\gamma d}$  decreases with increase in horizontal seismic coefficient by maximum 24.42%.
- 3)  $F_{\gamma d}$  decreases with increase in vertical seismic coefficient by maximum 27.52%.
- 4) Decrease in  $F_{\gamma d}$  is more significant with increase in  $k_v$ .
- 5)  $F_{\gamma d}$  increases marginally with increase in inclination of load and rate decreases with increases in  $k_h$  and  $k_v$ .
- 6)  $F_{\gamma d}$  increases significantly with increase in embedment ratio.

#### V. NOTATION

- $w_a$  = The weight of active failure wedge ABE, in active case,  
 $w_p$  = The weight of, failure wedge, CDF, in passive case,  
 $k_h$  = seismic coefficient's in horizontal direction,  
 $k_v$  = The seismic coefficient in vertical direction,  
 $\phi$  = Angle of internal friction,  
 $B$  = width of vertical strip anchor,  
 $H$  = height of vertical strip anchor below ground surface,  
 $R_a$  = The reaction exerted by the soil to the failure surface AE,  
 $R_p$  = The reaction exerted by the soil to the failure surface DF,  
 $\alpha_a$  = . an angle made by failure surface in active case ,  
 $\alpha_p$  = . an angle made by failure surface in passive case.

#### REFERENCES

- [1] Akinmusuru, J. O. (1978). "Horizontally loaded vertical anchor plate in sand." J. Geotech. Engg.Div., ASCE, 104(2), pp- 283-286.
- [2] Bhardwaj, S. and Singh, S.K, (2014). "Ultimate capacity of battered micropiles under oblique pullout loads." J.Geotech. Engg, 9(2), pp-190-200.
- [3] Basudhar, P. K., and Singh, D. N., (1994). " A generalized procedure for predicting optimal lower bound break-out factors of strip anchors." Geotechnique, 44(2), pp-307-318.

- [4] Bhattacharya, P. and Kumar, J., (2012). "Seismic pullout capacity of vertical anchors in sand." Geomechanics and Geoengeering, 8(3), pp-191-201.
- [5] Choudhury, D., and Nimbalkar, S., (2007). "Seismic rotational displacement of gravity walls by pseudo-dynamic method: Passive case." Soil Dyn. Earthquake Eng., 27(3), pp-242-249.
- [6] Choudhury, D., and Nimbalkar, S. S., (2008). "Seismic rotational displacement of gravity walls by pseudo-dynamic method." Int. J. Geomech., 8:3(169), pp-169-175.
- [7] Das, B. M., (1990). "Earth Anchors."Elsevier, Amsterdam, Oxford, Newyork, Tokyo.
- [8] Das, B. M., (1979). "Pullout Resistance of Vertical Anchors."(Journal of the Geotechnical Engineering Division, ASCE, 101,( GT1), pp. 87-91.
- [9] Das, B. M., and Seeley, G. R., (1975). "Load-displacement relationship for vertical anchor plates." J. Geotech. Engg., ASCE, 101(7), pp-711-715.
- [10] Dickin, E. A., and Leung, C. F., (1983). "Centrifuge model tests on vertical anchor plates."J. of Geotech. Eng., 109(12) pp-1503-1525.
- [11] Dickin, E., A., and Leung, C., F., (1985). "Evaluation of design methods for vertical anchor plates." J.Geotech. Eng., ASCE, 111(4), pp-500-520.
- [12] Ghaly A. (1997). Load-displacement prediction for horizontally loaded vertical plates.J Geotech Geoenviron Eng;123(1):74-6.
- [13] Ghosh, P., (2009). "Seismic vertical uplift capacity of horizontal strip anchors using pseudo-dynamic approach." Comp. Geotech., 36(1-2), pp-342-351.
- [14] Kame,G.S.,Dewaikar D.M.,Choudhury,D., (2012). "Pullout Capacity of a Vertical Plate Anchor Embedded in Cohesion-less Soil."Canadian Center of Science and Education, 1,pp 27-56.
- [15] Khan, A. J., Mostofa, J. and Jadid, R. (2017), " Pullout Resistance of concrete anchor block embedded in coheionlesssoil", Geomechanics and Engineering,12 (4),
- [16] Kramer, S.L. (1996). "Geotechnical Earthquake Engineering." Prentice Hall,UpperSaddle River, NJ.
- [17] Kumar, J., (2002). "Seismic horizontal pullout capacity of vertical anchors in sand." Canadian Geotechnical Journal, 39(4), pp-982-991.
- [18] Kumar, J. and Rao, M.V.B.K., (2004). Seismic horizontal pull-out capacity of shallow vertical anchors in sand. Geotechnical and Geological Engineering, 22, 331-349.
- [19] Merifield, R.S., Sloan, S.W., (2006). "The Ultimate Pullout Capacity of Anchors in Frictional Soils." Canadian Geotechnical Journal, 43(8), pp-852-868.
- [20] Nazir, R., Chuan, H. S., Niroumand, H., & Kassim, K.,A.,(2014) "Performance of Single Vertical Helical Anchor Embedded in Dry Sand." Elsevier, 49, pp-42-51.
- [21] Neely, W. J., Stuart, J. G., and Graham, J., (1973) "Failure Loads of Vertical Anchor Plates in Sand."Journal of the Soil Mechanics and Foundations Division, ASCE, 99(9), pp- 669-685.